AUTOMATYKA

COMPLEX-HARMONIC ANALYSIS OF ELECTRIC CIRCUIT CONTAINING A VIBRATING-PLATE CAPACITOR

Andrey Tyavlovsky, Anatoly Zharin
Byelorussian National Technical University, Minsk, Belarus

Abstract. *A complex-harmonic analysis technique was used for mathematical analysis of electric circuit containing a vibrating-plate capacitor. An equation for the transducer function of such a circuit is obtained. Amplitude and phase frequency characteristics of a circuit were calculated using a MathCAD program. Recommendations on implementation of a different frequency characteristic's parts in a measurement system design are formulated on a basis of graphical analysis.*

Keywords: non-linear circuit, vibrating-plate capacitor, frequency characteristics, complex-harmonic analysis

Analiza widmowych składowych zespolonych obwodu elektrycznego zawierającego kondensator z wibrującą okładką

Streszczenie. *Technika analizy zespolonych składowych widmowych została wykorzystana do matematycznej analizy obwodu elektrycznego zawierającego kondensator z wibrującą okładką. Otrzymano funkcję przetwarzania takiego układu. Amplitudy i fazy charakterystyki częstotliwościowej takiego układu obliczono przy użyciu programu MathCAD. Na podstawie graficznej analizy sformułowano zalecenia dotyczące stosowania różnych części charakterystyki częstotliwościowej w konstrukcji układu pomiarowego.*

Słowa kluczowe: obwody nieliniowe, kondensator z wibrującą okładką, charakterystyka częstotliwościowa, analiza zespolonych składowych widmowych

Introduction

Vibrating-plate capacitors are often used in such devices as capacitor microphones, micromechanical accelerometers, Kelvin probe electrometers etc. Performance and metrological characteristics of measuring instrument containing a vibrating-plate capacitor depends on transducer characteristic of the latter. So the defining of this characteristic is an important task in the field of measuring instruments development. This matter is of particular interest in contact potential difference (c.p.d.) measurements which are commonly held via using a vibrating capacitor Kelvin probe [4]. In such case input signal is surface potential or c.p.d. which can be expressed as DC voltage and output signal is AC voltage. Difficulties in calculation of vibrating-plate capacitor`s transducer characteristic are tied with non-linear character of differential equation that describes a corresponding circuit [1]. It makes a solution of this equation highly non-trivial.

To solve this problem an implementation of complex-harmonic analysis is proposed. This approach will simplify an analysis of highly non-linear circuit and allow calculating a complex transducer factor of electric circuit containing a vibrating-plate capacitor as well as phase-frequency characteristics of such a circuit. Results of such calculation can be used as basis for proposals on improvement of transducer's characteristics.

1. Complex-harmonic model of a circuit containing a vibrating-plate capacitor

The vibrating-plate capacitor, also known as Kelvin probe, is a parallel-plate capacitor where one plate is moving in respect to another in periodical manner. In the most common case of harmonic oscillations of capacitor's plate a gap between these two plates can be expressed as:

$$d(t) = d_0 - d_1 \cos \omega t\,, \tag{1}$$

where d_0 is an average gap between plates (a gap without vibration applied); d_1 is vibration amplitude; ω is vibration circular frequency; and t is time.

Let's implement modulation factor $m = d_1 / d_0$. The equation (1) can be rewritten in the form:

$$d(t) = d_0 (1 - m) \cos \omega t\,. \tag{2}$$

So the electrical capacity between two plates of vibrating-plate capacitor can be expressed as:

$$C(t) = \frac{\varepsilon\varepsilon_0 A}{d(t)} = C_0 \frac{1}{1 - m\cos\omega t} \tag{3}$$

where ε is relative electrical permittivity of media between plates (ε = 1 in the case of vacuum and $\varepsilon \approx 1$ in the case of air); $\varepsilon_0 = 8{,}85 \cdot 10^{-12}$ is absolute electrical permittivity of vacuum; A is plate's area (an area of a smallest plate in a case of non-equal plates; in a particular case of Kelvin probe A is a probe's tip geometrical area); and C_0 is an average capacity of vibrating-plate capacitor.

In a measuring device a vibrating-plate capacitor always acts as an element of some electrical circuit. In the most common case this circuit includes, besides vibrating-plate capacitor, an input impedance Z_{in} of a cascade next to vibrating-plate capacitor. Considering Z_{in} as a fully active resistance (which is correct for most practical cases) we may substitute it by active resistor R_{in}. Measurement signal acts as a voltage between capacitor's plates, so in a substitution scheme that is shown in Fig. 1 there must be a voltage source V_C coupled with a vibrating-plate capacitor $C(t)$ in a successive manner.

In a presence of electrical charge on capacitor's plates a modulation of capacity as expressed in (3) will produce an electrical current $i(t)$ in the circuit. Under the Kirchhoff's rules, the equation for voltages and currents in a given circuit must be:

$$V_c = i(t) R_{in} + V(t), \tag{4}$$

where $V(t)$ is output AC signal due to modulation of capacity as mentioned above.

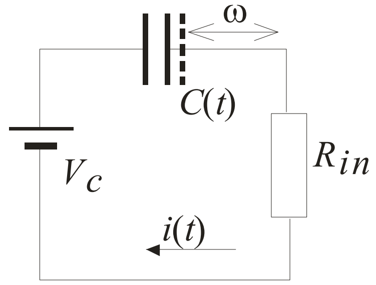

Fig. 1. Substitution electrical scheme of a measuring device with a vibrating-plate capacitor.
Rys. 1. Elektryczny schemat zastępczy układu pomiarowego z kondensatorem z wibrującą okładką.

This equation can be rewritten in differential form:

$$\frac{V_c}{R_{in}} = \frac{dQ(t)}{dt} + \frac{Q(t)}{R_{in} C(t)}, \tag{5}$$

where $Q(t)$ is electrical charge on vibrating-plate capacitor's plates.

Artykuł recenzowany *otrzymano: 27.02.2012r., przyjęto do druku: 1.03.2012r.*

The main problem in solving the equation (5) is ultimately non-linear character of $C(t)$ which is defined by the equation (3).

The capacity $C(t)$ can be expressed as a sum of static capacity C_0 and its deviation $\Delta C(t)$:

$$C(t) = C_0 + \Delta C(t). \tag{6}$$

The capacity deviation can be found by substitution of C_0 from (3). The result is:

$$\Delta C(t) = \frac{mC_0 \cos\omega t}{1 - m\cos\omega t}. \tag{7}$$

This equation is not a classic harmonic function, and the degree of non-linearity increases with increasing of modulation factor m. Graphical representation of function $\Delta C(t)$ for some m meanings is given in Fig. 2.

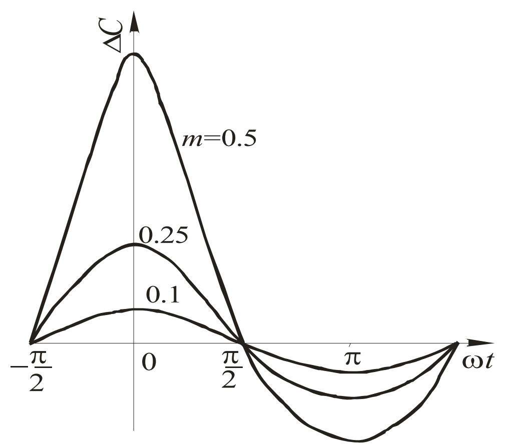

Fig. 2. Capacity deviation vs vibration angular phase ωt for different meanings of modulation factor m. Y axis scale is in conventional units.
Rys. 2. Zmiana pojemności w zależności od kąta fazowego wibracji ωt dla różnych wartości głębokości modulacji m. Na osi Y jednostki umowne.

It can be clearly seen that $\Delta C(t)$ vs ωt graph becomes highly nonsymmetrical with $m > 0{,}1$. It means that $C(t)$ proceeds in nonsymmetrical manner as well and particularly that static capacity C_0 can not be determined as mean value of $C(t)$.

To solve the equation (5) with function $C(t)$ determined by (6) and (7) we may integrate it using an integration scaling factor μ which is determined by:

$$\mu = \exp\left(\int \frac{1}{R_{in}C(t)}dt\right). \tag{8}$$

It leads to a generic solution in the following form:

$$Q(t) = \frac{V_C}{R_{in}} \exp\left(-\frac{t}{R_{in}C_0} - \frac{m}{\omega R_{in}C_0}\cos\omega t\right) \times \int_0^t \exp\left(\frac{t}{R_{in}C_0} - \frac{m}{\omega R_{in}C_0}\cos\omega t\right)dt. \tag{9}$$

This solution is practically useless because of impossibility to express an integral like $\int_0^t \exp\left(\frac{t}{R_{in}C_0} - \frac{m}{\omega R_{in}C_0}\cos\omega t\right)dt$ via elementary functions.

So the common approach employed particularly by D.M. Taylor [3], is to use an approximate equation:

$$\frac{V(t)}{V_C} \approx \frac{\Delta C}{C_0} \approx \frac{d_1}{d_0}. \tag{10}$$

This approximation is only valid for very large time constant of input circuit $R_{in}C_0 \geq \frac{2\pi}{\omega}$ which is rarely observed in measurement practice. Moreover, many applications (like capacitive microphones, rapid measurement systems etc.) require ultimately small time constant. So we need to found a generic solution of (9) without this simplification.

So far it was decided to use a method of complex harmonic analysis developed by G.E. Puchov [2].

The method is based on finite limits Laplace and Fourier transformations which are given as:

$$F_n^* = j\frac{2}{T}\int e^{-jn\omega t} f(t)dt, \tag{11}$$

where F_n^* is a complex image of a real argument function $f(t)$ that represents a complex amplitude of function's n^{th} harmonic (n = 0, 1, 2, …) on a time section [0, T]; T is a period where function $f(t)$ is measured; and j is an imaginary unit.

Using a transitional operator K_n which describes a transition from a real pre-image to it's complex image we can write $F_n^* = K_n\left[f(t)\right]$.

The reverse transformation from a complex image to a real pre-image can be made just by summing of a trigonometrical Fourier row:

$$f(t) = \frac{1}{2j}\sum_{n=-\infty}^{\infty} F_n^* e^{-jn\omega t} = \frac{F_0}{2j} + \sum_{n=1}^{\infty} F_n \sin(n\omega t + \varphi_n), \tag{12}$$

where F_n and φ_n are amplitude and phase of function $f(t)$ n^{th} harmonic respectively. They can be calculated as:

$$F_n = \sqrt{(\mathrm{Re}\,F_n^*) + (\mathrm{Im}\,F_n^*)^2} \tag{13}$$

and

$$\varphi_n = arctg\frac{\mathrm{Im}\,F_n^*}{\mathrm{Re}\,F_n^*}, \tag{14}$$

where $\mathrm{Re}\,F^*_n$ and $\mathrm{Im}\,F^*_n$ are real and imaginary part of complex number F_n^* respectively.

We can apply (11) to the equation (7) taking a period of vibrating-plate capacitor's oscillations $T = \frac{2\pi}{\omega}$ as integration limits. In accordance with employed definitions, a complex image of function $Q(t)$ can be written as $K_n\left[Q(t)\right] = Q_n^*$. Consequently, image of derivation of this function will be:

$$K_n\left[\frac{Q(t)}{dt}\right] = jn\omega Q_n^*. \tag{15}$$

Taking into account the rule of multiplication of a pre-image on a constant we can write:

$$K_n\left[\frac{1}{R_{in}}\frac{Q(t)}{C(t)}\right] = \frac{1}{R_{in}}K_n\left[\frac{Q(t)}{C(t)}\right] \tag{16}$$

and

$$K_n\left[\frac{U_C}{R_{in}}\right] = \frac{U_C}{R_{in}}K_n\left[1\right], \tag{17}$$

where $K_n\left[1\right]$ is a complex image of a unit function:

$$K_n\left[1\right] = \begin{cases} j2, n = 0 \\ 0, n \neq 0 \end{cases}. \tag{18}$$

Using the conditional term $\frac{1}{C(t)} = N$ we get:

$$K_n\left[\frac{1}{C(t)}\right] = K_n\left[N\right] = N_n^*. \tag{19}$$

An image of two functions' product can be written as [4]:

$$K_n\left[\frac{1}{C(t)}Q(t)\right] = \frac{1}{j2}\sum_{\nu=-\infty}^{\infty} N_{n-\nu}^* Q_\nu^* = \frac{1}{j2}\sum_{\nu=-\infty}^{\infty} N_\nu^* Q_{n-\nu}^*. \tag{20}$$

Taking into account expressions (15), (16) and (20) we can obtain a complex image of the equation (6) in a form of a system of algebraic equations which can be written as following:

$$jn\omega Q_n^* + \frac{1}{j2R_{in}}\sum_{\nu=-\infty}^{\infty} N_\nu^* Q_{n-\nu}^* = \frac{U_C}{R_{in}}K_n\left[1\right]. \tag{21}$$

Coefficient $C(t)$ from equation (3) can be substituted into equation (20). Next, implementation of transformation (11) gives us:

$$N_n^* = \begin{cases} \frac{j2}{C_0}, \nu = 0 \\ -\frac{jm}{C_0}, \nu = 0. \\ 0, \nu \neq 0 \end{cases} \qquad (22)$$

Substitution of N_n^* from (22) and $K_n[1]$ from (18) together with use of an image's feature $Q_{-n}^* = .-Q_n^*$ [2] gives us:

$$Q_0^* = .\frac{j2U_C C_0}{1-\frac{m}{2}\frac{Q_1^* - \hat{Q}_1}{Q_0^*}},$$

$$Q_n^* = .\frac{m}{2}\frac{Q_{n-1}^* + Q_{n+1}^*}{1 jn\omega R_H C_0 + 1}, \qquad (23)$$

where $\hat{Q}_1$ is a complex coupled to Q_n number.

The solution of (23) with respect to (12)-(14) is an infinite sum of harmonics which can be expressed as:

$$Q(t) = Q_0 + Q_1\sin(\omega t + \varphi_1) + Q_2\sin(\omega t + \varphi_2) + \\ + \ldots + Q_n\sin(\omega t + \varphi_n) + \ldots. \qquad (24)$$

For practical purposes we need to cut this row by some finite number of n harmonics. Therefore the solution obtained will not be the exact one, but we can reduce a calculation error to any desired limit by proper selection of n making it acceptable for engineering purposes [5].

A response of a measuring system containing a vibrating-plate capacitor can be found by differentiation of equation (24). A result of differentiation gives us a current in the circuit. Consequently, a voltage response of a measuring system can be found from Ohm's law via multiplying it on load resistance R_{in}. A transducer factor can be calculated by dividing of output voltage $U(t)$ by input voltage U_C as $A = \frac{U(t)}{U_C}$. After calculations we obtain:

$$A = \frac{U(t)}{U_C} = \frac{Q_1\omega R_{in}}{U_C}\sin(\omega t + \varphi_1) + \\ + \frac{2Q_2\omega R_{in}}{U_C}\sin(2\omega t + \varphi_2) + \ldots + \\ + \frac{nQ_n\omega R_{in}}{U_C}\sin(n\omega t + \varphi_n). \qquad (25)$$

All the Q_i meaning can be calculated from (23) for any set of circuit's parameters. The equation (25) gives us a transducer function of electric circuit containing a vibrating-plate capacitor which was effectively resolved by complex-harmonic analysis technique.

2. Numerical analysis of amplitude and phase frequency performance of a circuit with vibrating-plate capacitor

In most applications it's necessary to know a complex frequency response of a given circuit. Another task, closely related to the former, is optimization of circuit parameters to obtain a desired frequency characteristic. From this point of view, we can use equations (23) and (25) for mathematical modeling of circuit's behavior with respect to its parameters. As these we can choose a vibrating-plate capacitor's static capacity C_0, a load resistivity R_{in}, a vibration frequency ω, and a modulation factor m. We used a standard MathCAD program to calculate corresponding amplitude-frequency and phase-frequency characteristics. Graphical results of calculations are given in Fig. 3. Plots are made in logarithmical scale.

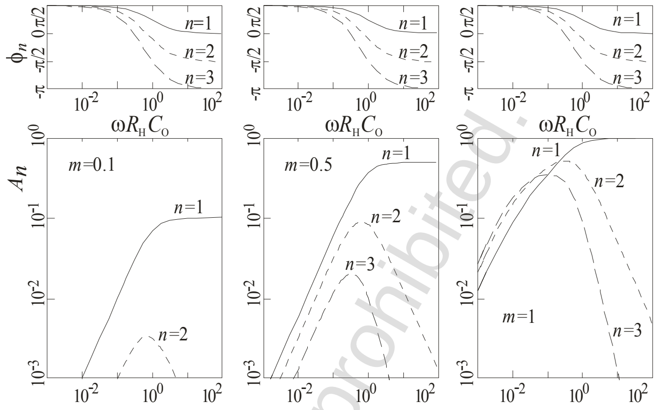

n is harmonic's number; *m* is modulation factor.

Fig. 3. Normalized amplitudes and phases of output signal of a circuit containing a vibrating-plate capacitor as a function of normalized frequency $\omega R_H C_0$ for different modulation factor values.

Rys. 3. Znormalizowane amplitudy i fazy wyjściowego sygnału układu z kondensatorem z wibrującą okładką w funkcji częstotliwości znormalizowanej $\omega R_H C_0$ dla różnych wartości współczynnika modulacji.

The resulting plots are clearly divided into three segments with different amplitude and phase combinations on each. They can be characterized as following:

Segment 1: a low-frequency segment where $\omega R_H C_0 \leq 0{,}1$. Phases of first three harmonics in this part are roughly equal, all about $\varphi_n \approx \pi/2$. Normalized amplitudes of these harmonics are raises in monotonous manner with frequency increases. Higher harmonics are expressed significantly here resulting in a high distortion factor value. Therefore the circuit itself can be characterized as significantly non-linear on low frequencies. However, in some applications it can be judged as a positive feature. For example, Kelvin probe measuring system with unshielded electromagnetic or electrostatic actuator will generate noise on an actuator's frequency. To improve SNR (signal-to-noise ratio) one could use a second or higher harmonic of a signal, which is considerably strong on low frequencies, and a rejection filter to suppress a noised first harmonic.

Segment 2: a medium-frequency segment where $0{,}1 \leq \omega R_H C_0 \leq 10$. It's a transitional section where phases of all the harmonics are changing continuously with frequency, but with different slopes. It means that harmonic distortion factor value will be high and unstable with frequency. In line with it, amplitudes of harmonics demonstrate different behavior in this segment. The first harmonic changes its slope from positive to zero, becoming then constant with frequency. The second and the third harmonics reach their particular maximums in this segment than gaining a negative slope, therefore becoming descending. High and instable value of harmonic distortion factor makes this segment of frequency characteristic unsuitable for practical purposes in measuring instruments development.

Segment 3: a high-frequency segment where $\omega R_H C_0 \geq 10$. On high frequencies the first harmonic becomes dominant while other harmonics descent quickly with frequency. The descent rate grows with harmonic's number, so the harmonic distortion factor value lowers. Phase shifts became different but constant for each harmonic, getting values $\varphi_2 \approx -\pi/4$, $\varphi_3 \approx -3\pi/4$. The first harmonic keeps its phase shift at zero level, $\varphi_1 \approx 0$. Therefore this segment of frequency characteristic is preferable for measuring systems working on the first harmonic of output signal.

It's notable that amplitudes of all the harmonics rise quickly with modulation factor m. The raise is more pronounced for higher harmonics, so the harmonic distortion factor lowers with modulation factor growth. Moreover, when $m \to 1$ amplitudes of the second and even of the third harmonics become higher than that of the first harmonic. Again, this mode can be used when developing a system working on high harmonics of a signal. On other hand, high sensitivity of these harmonics to modulation factor value requires a thorough handling of a probe-to-surface gap.

1. Conclusions

1. A transducer function of electric circuit containing a vibrating-plate capacitor is obtained using a complex-harmonic analysis technique. An analytical solution of corresponding equation is obtained in the form of an infinite sum of harmonics, so it can't be used as an exact solution in engineering practice. Nevertheless, this row can be cut by some finite number *n* of harmonics giving a certain calculation error which can be reduced to any desired limit by proper selection of *n*.

2. A numerical calculation of amplitude- and phase-frequency characteristics of a circuit containing a vibrating-plate capacitor gives us three distinguishable segments. In a low-frequency segment normalized amplitudes of the first three harmonics are raises in monotonous manner with frequency increases. Higher harmonics are expressed significantly here resulting in a high distortion factor value. A medium-frequency segment is characterized by rapid change of all the harmonics' phases with frequency. The second and the third harmonics reach their particular maximal values here. In a high-frequency segment the first harmonic becomes dominant while other harmonics descent quickly with frequency.

3. The results of calculations show that the raise of modulation factor *m* leads to the raise of all the harmonics' amplitudes. The effect is more pronounced for higher harmonics, so the distortion factor increases for higher *m* meanings.

4. Recommendations on the results of analysis and calculations could be the following. A low-frequency ($\omega R_H C_0 \le 0{,}1$) segment of frequency characteristics is characterized by strong distortion factor and therefore can be used for measurements on a second or higher harmonic of a signal, that can improve a signal-to-noise ratio by a rejection of a noised first harmonic. A medium-frequency ($0{,}1 \le \omega R_H C_0 \le 10$) segment is non-preferable for any measurement purposes due to high sensitivity of an output signal to small frequency shifts, gaining a high measurement error. In contrast to it, a high-frequency ($\omega R_H C_0 \ge 10$) segment is preferable for measurements on the first harmonic of a signal. This part is characterized by least frequency dependence of a first harmonic and rapid lowering of higher harmonics with frequency. For the higher sensitivity of a measurement system a modulation factor *m* could be greatened, but the high sensitivity of the second and higher harmonics to modulation factor value requires a thorough handling of a probe-to-surface gap in this mode.

References

[1] Lonardo, P. M., D. A. Lucca, et al. *Emerging Trends in Surface Metrology* // CIRP Annals - Manufacturing Technology. – 2002. – № 51(2). – P. 701-723.

[2] Пухов, Г. Е. *Комплексное исчисление и его применение*. – Киев: Из-во АН УССР, 1961. – 220 с.

[3] Taylor, D. M. *Measuring techniques for electrostatics* // Journal of Electrostatics. – 2001. – № 51-52. – P. 502-508.

[4] Zharin, A. L. *Contact Potential Difference Techniques as Probing Tools in Tribology and Surface Mapping* // Scanning Probe Microscopy in Nanoscience and Nanotechnology (edited by B. Bhushan). – Springer Heidelberg Dordrecht London New York, 2010. – P. 687-720.

[5] Zharin, A. L., Tyavlovsky, A.K. *Electronic Work Function as a Parameter for Materials Characterization and On-line Surface Monitoring* // Optical and nanotechnology for the materials in science and life: Proceedings of International conference (15-19 June 2010). – Minsk: Kovcheg, 2010. – V. 2. – P. 82-97.

Ph.D. Andrey K. Tyavlovsky
e-mail: andrey_psf@tut.by

Andrey K. Tyavlovsky graduated from Byelorussian State Politechnical Academy in 1999. He worked as an engineer-metrologist at the City's Emergency Hospital of Minsk. The same year he joined a post-graduate scholarship of the BSPA. In 2003 he earned a Ph.D. degree on Metrology. Now he works at Byelorussian National Technical University as a lecturer and research worker. Area of interests includes electrochemistry, surface properties study and electronics.

Dr. Anatoly L. ZHARIN
e-mail: anatoly.zharin@gmail.com

Dr. Anatoly L. Zharin graduated from Gomel State University, in 1972. He worked at the Belarussian State University, the Belarussian State Research and Production Powder Metallurgy Concern, the Georgia Institute of Technology (USA), the Byelorussian National Technical University. Dr. Zharin's research interests include experimental techniques, electronics and computer techniques with applications to experimental studies of friction and wear processes.